

Iterative Symbol Offset Correction Algorithm for Coherently Modulated OFDM Systems in Wireless Communication

V.S. Abhayawardhana, I.J. Wassell

{vsa23,ijw24}@eng.cam.ac.uk

Laboratory for Communications Engineering,
Department of Engineering, University of Cambridge, UK

Abstract—Orthogonal Frequency Division Multiplex (OFDM) system performance remains acceptable under timing synchronisation errors as long as the start of each symbol is determined to lie within a certain length into the Cyclic Prefix (CP). The Schmidl and Cox Algorithm (SCA) is quite robust in estimating the timing and frequency offset synchronisation for systems with large OFDM symbol lengths. It uses two OFDM symbols for training with the first one having two identical halves. The start of the frame is estimated by correlating a received sequence of samples equal to half the OFDM symbol length with the following received samples. The effect of Additive White Gaussian Noise (AWGN) in the estimation process is mitigated only if the number of samples used in the correlation, and hence the OFDM symbol size is large. However to be successfully applied to Broadband Fixed Wireless Access (BFWA) systems, OFDM should perform well even with smaller symbol lengths. In this paper we present the Iterative Symbol Offset Correction Algorithm (ISOCA), which uses the SCA for initial coarse timing synchronisation and follows it with a two stage symbol offset correction algorithm by tracking the phase of the second training symbol. We show through simulation that the ISOCA achieves virtually perfect estimation of the Start of Frame (SOF), even with very low received SNR.

Keywords—OFDM, symbol offset, Schmidl and Cox algorithm, BFWA

I. INTRODUCTION

Orthogonal Frequency Division Multiplexing (OFDM) has become increasingly popular for wireless data transmission in Broadband Fixed Wireless Access (BFWA) systems due to its robustness under multipath effects. The modulated subcarriers overlap spectrally, but since they are orthogonal over a symbol duration, they can be easily recovered as long as the channel does not destroy the orthogonality. The orthogonality of the consecutive OFDM symbols is maintained in a time dispersive channel by appending a length v cyclic prefix (CP) at the start of each symbol. The CP is obtained by taking the last v samples of each symbol and consequently the total length of the transmitted OFDM symbols is $(N + v)$ samples. For each OFDM symbol to be independent and to avoid any Inter Symbol Interference (ISI) or Inter Carrier Interference (ICI), the number of samples spanned by the Channel Impulse Response (CIR), N_h should be less than $v + 1$ samples. Hence the distortion caused by the CIR only affects the samples within the CP. The receiver discards the CP and takes only the last N samples of each OFDM symbol for demodulation by the receiver FFT. Consequently, for coherently modulated OFDM systems the effects of the CIR can then be equalized by an array of one-tap Frequency Domain Equalizers (FEQ) following the FFT.

Unfortunately, OFDM has been proven to be very sensitive to carrier frequency offset and phase noise caused by tuning oscillator inaccuracies or Doppler shifts induced by the channel. However OFDM is quite robust against timing synchronisation errors, which can be further divided into symbol synchronisation errors and sampling clock synchronisation errors. The purpose of the symbol synchronisation is to find the correct position of the FFT

window required for demodulation. In this paper we consider that perfect sampling clock synchronisation is achieved. In practice, the length of the CP, v is selected to be slightly longer than the length of the CIR, N_h . Hereafter we will denote this difference as Excess Length, p (i.e. $p = v - N_h$). As long as the symbol synchronisation offset, ξ causes the start of each FFT window to lie within the Excess Length (i.e. $-p \leq \xi \leq 0$), the decoded OFDM symbols will not be subjected to Inter Block Interference (IBI). In the interests of efficiency, it is desirable to keep p as small as possible.

For a BFWA system a single base station (BS) will transmit data in short bursts to many subscriber units (SUs). Consequently, a system with large value of N is not practical and in the interests of transmission efficiency, a robust symbol synchronisation algorithm capable of operating with a very small Excess Length is required.

The algorithms that are already available for symbol synchronisation can be broadly categorised into Pilot Symbol Aided (PSA) and Non Pilot Symbol Aided (NPSA) schemes. PSA schemes are based on correlating the received signal with a known signal. These can be further divided into ones that use a preamble or a known OFDM training symbol [1] or ones that periodically insert pilot symbols on particular subchannels [2]. NPSA schemes are generally based on correlating received samples taken one OFDM symbol length apart, utilising the periodicity created by the insertion of the CP [3]. Some schemes however employ a hybrid of PSA and NPSA methods. [4].

This paper is organised as follows, section II studies analytically the effect of symbol synchronisation errors in OFDM. Section III briefly introduces the Schmidl and Cox Algorithm (SCA)[1], which is one of the more robust schemes for symbol synchronisation and section IV introduces the novel Iterative Symbol Offset Correction Algorithm (ISOCA) that compliments the SCA and improves the performance. Section V shows results obtained by computer simulation and section VI concludes and proposes future work.

II. EFFECT OF SYMBOL OFFSET IN OFDM

All analysis and simulations in this paper are performed in the digital complex baseband domain. The n th sample of the m th OFDM symbol generated by the Inverse FFT (IFFT) at the transmitter is

$$s_{m,n} = \sqrt{\frac{1}{N}} \sum_{k=0}^{N-1} A_{m,k} e^{j2\pi \frac{kn}{N}}, \quad 0 \leq n \leq N-1 \quad (1)$$

$A_{m,k}$ is the data symbol modulated on to the k th subcarrier of the m th OFDM symbol. The data is con-

verted into a serial sequence, then the CP of length v is added. Thus the m th transmitted OFDM symbol is $\underline{s}(m) = [s_{m,N-v}, \dots, s_{m,N-1}, s_{m,0}, \dots, s_{m,N-1}]^T$. We assume a finite length CIR with N_h samples, $\underline{h} = [h_0, \dots, h_{N_h-1}]^T$, where $v \geq N_h - 1$. The received sequence can be expressed as $r_n = (s_n * h_n)$ where s_n are serially concatenated transmitted symbols, $\underline{s}(m)$.

At the receiver, samples corresponding to the CP are discarded and the remaining samples of the active OFDM symbol are used for decoding. The symbol after FFT demodulation is

$$Y_{m,l} = \sqrt{\frac{1}{N}} \sum_{n=0}^{N-1} (r_{m,n} + w_n) e^{-j2\pi \frac{ln+(\epsilon-\hat{\epsilon})}{N}}, 0 \leq l \leq N-1 \quad (2)$$

where $r_{m,n}$, $0 \leq n \leq N-1$ are the received samples of the FFT window for the m th OFDM block taken from r_n , as determined by the symbol synchronisation algorithm and w_n is the component due to Additive White Gaussian Noise (AWGN). Here ϵ is the carrier frequency offset relative to the intercarrier spacing and $\hat{\epsilon}$ represents the estimated carrier frequency offset at the receiver. We will assume $\hat{\epsilon} - \epsilon = 0$ for the remainder of this section in order to analyse the effect of symbol offset errors. Hence,

$$Y_{m,l} = A_{m,l} H_l + W_l \quad (3)$$

where H_l is the transfer function of the channel at the subchannel index l and W_l is the component due to AWGN. To understand the effect of symbol offset on the performance, we look at the result of the decoded OFDM symbols subjected only to AWGN for two different cases of symbol offset, ξ .

A. Symbol Offset $-v \leq \xi < 0$

In this case, the FFT window selected for decoding is $\underline{r}_m = [r_{m,N-\xi}, \dots, r_{m,N-1}, r_{m,0}, \dots, r_{m,N-1-\xi}]$

$$Y_{m,l} = \frac{1}{N} \sum_{k=0}^{N-1} A_{m,k} \sum_{n=0}^{\xi-1} e^{j2\pi \frac{k(n+N-\xi)-nl}{N}} + \frac{1}{N} \sum_{k=0}^{N-1} A_{m,k} \sum_{n=\xi}^{N-1} e^{j2\pi \frac{k(n-\xi)-nl}{N}} + W_l \quad (4)$$

and hence

$$Y_{m,l} = A_{m,l} e^{j2\pi \frac{\xi l}{N}} + W_l \quad (5)$$

As shown by equation (5), as long as the symbol offset forces the beginning of each FFT window to be selected within the CP, the orthogonality of the carriers is maintained.

B. Symbol Offset $\xi > 0$

Now $\underline{r}_m = [r_{m,\xi}, \dots, r_{m,N-1}, r_{m+1,N-v}, \dots, r_{m+1,N-v-1+\xi}]$. After similar analysis we obtain,

$$Y_{m,l} = \frac{N-\xi}{N} A_{m,l} e^{j2\pi \frac{\xi l}{N}} + \frac{1}{N} \sum_{k=0}^{N-1} A_{m,k} \sum_{n=0}^{N-\xi-1} e^{j2\pi \frac{k(n+\xi)-nl}{N}} + \frac{1}{N} \sum_{k=0}^{N-1} A_{m+1,k} \sum_{n=N-\xi}^{N-1} e^{j2\pi \frac{k(n+\xi-v)-nl}{N}} + W_l \quad (6)$$

The first rhs term of equation (6) shows the desired term experiencing an attenuation. The second and the third term are the ICI and ISI respectively. The analysis can be extended to the case when the OFDM symbols are also subjected to a representative CIR, in which case unless the symbol offset lies within $-p \leq \xi \leq 0$, the decoded symbols are given by,

$$Y_{m,l} = \frac{N-\xi}{N} A_{m,l} H_l e^{j2\pi \frac{\xi l}{N}} + W_{\xi,l} + W_l \quad (7)$$

where, $W_{\xi,l}$ is the interference term caused by ISI and ICI. This term also proves to be the dominant source of interference, which can be approximated by Gaussian noise with a finite power [5]. The important point that should be noted from equations (4)-(7) is that, the decoded OFDM symbols will always contain a phase rotation proportional to the symbol offset, ξ and the subchannel index, l as given by the term $e^{j2\pi \frac{\xi l}{N}}$. In the next two sections, we present an algorithm that uses this phase rotation to determine and correct the symbol offset.

III. SCHMIDL AND COX ALGORITHM (SCA)

A robust scheme to estimate both symbol synchronisation and frequency offset estimation is the SCA. It uses two training symbols with the first one having a repetition within half a symbol period. The frame synchronisation is achieved by searching for a training symbol with two identical halves. If $L = N/2$, the sum of L consecutive correlations between pairs of samples spaced L apart is found as,

$$P(d) = \sum_{n=0}^{L-1} (r_{d+n}^* r_{d+n+L}) \quad (8)$$

The timing metric generated via (8), reaches a peak at the end of the CP of the first training symbol [1]. The peak is actually maintained for a length equal to the Excess Length, $(p+1)$ just prior to the end of the CP of the first training symbol. Thus the correlator output will take the form of a plateau. It is assumed that the SCA has resulted in a condition of non acquisition if it is not possible to find such a plateau region.

Symbol synchronisation is achieved by locating the end of this plateau, denoted by d_{opt} . The Start of Frame (SOF) is determined as the start of first training symbol, given by $d_{opt} - v$. We will denote it as $\hat{\text{SOF}}_{SCA}$. The phase difference between the two halves of the first training symbol is caused by the frequency offset, $\phi = \pi\epsilon$. It can be estimated as $\hat{\phi} = 1/(p+1) \sum_{n=0}^p \angle P(d_{opt}-n)$. If $\epsilon < 1$ there is no phase ambiguity in $\hat{\phi}$ and the frequency offset can be estimated as, $\hat{\epsilon}_{SCA} = \hat{\phi}/\pi$. In order to resolve potential ambiguity use can be made of the second training symbol, as detailed in [1].

If $\hat{\text{SOF}}_{SCA}$ is different from the actual one, SOF_{ideal} it results in a symbol offset, ξ_{SCA} (i.e. $\xi_{SCA} = \hat{\text{SOF}}_{SCA} - \text{SOF}_{ideal}$). The effect of AWGN on the correct estimation of d_{opt} and hence $\hat{\text{SOF}}_{SCA}$ reduces with higher values of L , and hence the number of FFT points N , particularly when operating at low values of SNR. It has been shown that the SCA performs well for OFDM systems with N in excess of 1000 [1]. However, for BFWA systems, data is transmitted in short bursts, particularly in the uplink. In this situation, it would be wasteful to use an OFDM system

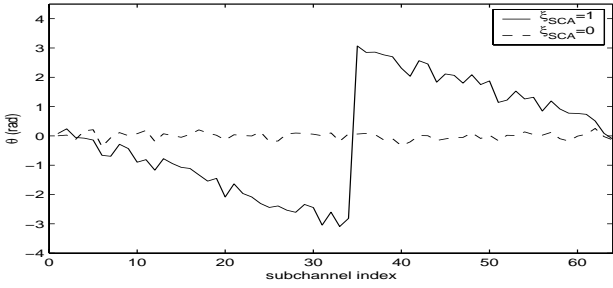


Fig. 1. Typical plots of θ for $N = 64$ at 15 dB SNR, $\epsilon = 0.5$ and $\xi_{SCA} = 0, 1$ with a CIR

with large N . Besides large values of N will give rise to the additional problems of high peak-to-average power ratio and will also introduce latency which reduces protocol efficiency. Typically BFWA systems utilise values of N in the range of 64 to 256. In this case, the estimate $\hat{\epsilon}_{SCA}$ is no longer sufficiently accurate resulting in a residual frequency offset that rotates the received constellation. Hence OFDM systems with low values of N will require a residual frequency offset correction algorithm to continuously track the carrier frequency offset. Some of these algorithms rely on the phase gradient of the decoded OFDM symbols to estimate the residual carrier frequency offset [6]. Even though $-p \leq \xi_{SCA} \leq 0$ will not result in any Inter Block Interference (IBI), the additional phase gradient caused by a non zero value of ξ_{SCA} will seriously affect the residual carrier frequency offset correction algorithms. Hence it is imperative that symbol synchronisation is achieved so that the final symbol offset, $\xi_F = 0$. In the next section we present the Iterative Symbol Offset Correction Algorithm (ISOCA), that employs a two step process that virtually guarantees perfect symbol synchronisation even under very low SNR conditions. An approach to increase the performance of the timing synchronisation of SCA is presented in [7], however only FFT sizes in excess of 1024 have been considered.

IV. ITERATIVE SYMBOL OFFSET CORRECTION ALGORITHM (ISOCA)

A. 1st Part - Iterative Symbol Offset Estimation

An initial estimate of both the SOF and ϵ , namely $\hat{\text{SOF}}_{SCA}$ and $\hat{\epsilon}_{SCA}$, are made using the SCA. We propose to estimate the symbol offset at the end of the SCA, ξ_{SCA} based on the phase gradient created as a result of it, as evident in equation (7). To do this, we utilise the decoded output of the second training symbol $Y_{N_{t2}}$. Here we have assumed that the two training symbols of the SCA occupy the symbol positions at the start of the frame, specifically N_{t1} and N_{t2} . We first calculate the phase difference between the received and the transmitted second training symbol of the SCA, as follows,

$$\theta = \angle(Y_{N_{t2}}/A_{N_{t2}}) \quad (9)$$

where $A_{N_{t2}}$ and $Y_{N_{t2}}$ represent the N_{t2} th transmitted and decoded symbols, respectively based on $\hat{\text{SOF}}_{SCA}$. Figure 1 shows a typical plots of θ against the subchannel index for $N = 64$, $\epsilon = 0.5$ and $\xi_{SCA} = 0$ and 1 subjected to a 3-tap SUI-2 CIR (which will be detailed in section V) with $v = 30$ and $p = 10$ and at an SNR of 15 dB. The frequency offset is corrected using

the estimation made using the SCA, $\hat{\epsilon}_{SCA}$. Any phase gradient present in θ when $\xi_{SCA} = 0$ is caused by the residual frequency offset, which is comparatively very small compared to that caused by the symbol offset, as seen from the Figure 1. Thus we can assume $\epsilon - \hat{\epsilon}_{SCA} \approx 0$ during the estimation of the symbol offset. Note that θ maintains a distinct gradient for non-zero values of ξ_{SCA} even when a representative CIR is included. However due to the phase wrapping effect, θ is first unwrapped by a suitable unwrapping algorithm. Since we are only interested in the phase gradient and not the exact phase values, a simple scheme was selected for the unwrapping of the phase [8]. For purposes of clarity, we denote the i th sample of the wrapped phase and the unwrapped phase as θ_i and $\hat{\theta}_i$, respectively. The phase unwrapping algorithm can be expressed as

$$\hat{\theta}_i = \hat{\theta}_{i-1} + \alpha \text{SAW}(\theta_i - \hat{\theta}_{i-1}) \quad (10)$$

where $\text{SAW}(\cdot)$ is a sawtooth function that limits the output to $\pm\pi$ and α is a parameter that controls the variance of the unwrapped phase. The estimate of the symbol offset is calculated as the gradient of the unwrapped phase $\hat{\theta}$.

$$\hat{\xi} = \text{ROUND}(\text{GRAD}(\hat{\theta}) \cdot N/2\pi) \quad (11)$$

where the $\text{GRAD}(\cdot)$ function finds the gradient of the best fit straight line fitted to the parameter in the least-squares sense and the $\text{ROUND}(\cdot)$ function rounds the parameter to the nearest integer. $\hat{\xi}$ is used to update the SOF. The estimate may not be accurate in the presence of channel impairments. Hence we propose to repeat the above process until $\hat{\xi} = 0$, updating the estimated SOF at the end of each iteration. (i.e. at the end of u th iteration $\hat{\text{SOF}}(u) = \hat{\text{SOF}}(u-1) + \hat{\xi}(u)$). We initialise the iterative process by letting $\hat{\text{SOF}}(0) = \text{SOF}_{SCA}$. It is found that in most cases the algorithm achieves the correct SOF within a few iterations even when a CIR is included. However at very low SNR values, there is a small probability of non-convergence. To prevent continual iteration, this condition is detected by allowing the algorithm to iterate only a predetermined number of times, N_{it} (i.e. $u \leq N_{it}$). In practice, this does not pose a big problem, as the receiver can always request a retransmission if convergence is not achieved. This is far more advantageous than estimating the SOF incorrectly and as a consequence obtaining samples comprising two OFDM received symbols in the FFT window. In this case the error rate will be very high.

B. 2nd Part - Error Comparison

Figure 2 shows how ISOCA works for two possible scenarios. The first is when $\xi_{SCA} < N/2$ as shown in Figure 2(a). The symbol offset correction is usually complete at the end of the iterative part of the ISOCA after u iterations. In the unlikely event that $\xi_{SCA} > N/2$, the gradient of θ actually changes sign. This will result in the unwrapping algorithm producing a gradient with the opposite sign to that required, which will subsequently cause the estimated symbol offset during iteration $\hat{\xi}$ to move away from SOF_{ideal} . In which case, when the iterative part terminates the estimated SOF will be more than $N/2$ samples away from the desired position as shown in Figure 2(b).

To address this situation, a second correction is made at the end of the iterative procedure. Here the decoded symbol output

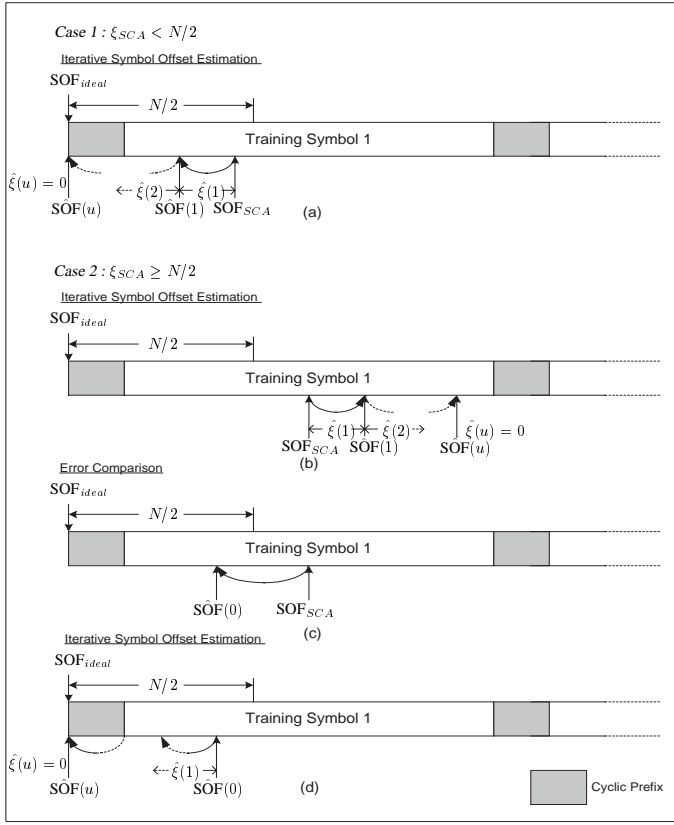


Fig. 2. Two Cases of ISOCA Correction

of the 2nd training symbol, $Y_{N_{t2}}$ is compared with the transmitted symbol, $A_{N_{t2}}$ based on the estimated SOF at end of iterative part, $\hat{SOF}(u)$. However, the results will be seriously affected by subchannels with a low SNR resulting from spectral nulls in the channel response H_l . To overcome this problem, an estimate of the channel response \hat{H}_l is made by comparing the transmitted and decoded output of the second training symbol.

$$\hat{H}_l = Y_{N_{t2}}/A_{N_{t2}} \quad (12)$$

Only those subchannels with $|\hat{H}_l|$ above a certain threshold are selected. We call this subset of subchannels $\underline{d} \subset [0, \dots, N-1]$. The chosen criteria selects only those subchannels with $|\hat{H}_l|$ in excess of a standard deviation above the mean. The outputs of these subchannels $\tilde{Y}_{N_{t2,d}}$ are sent through a slicer to obtain $\hat{Y}_{N_{t2,d}}$, where $d \in \underline{d}$. If the number of symbol errors between $\tilde{Y}_{N_{t2,d}}$ and $A_{N_{t2,d}}$ exceeds a predefined threshold, N_{er} it is assumed that the iterative estimation has diverged from the SOF_{ideal} . Otherwise it is assumed that ideal symbol synchronisation is achieved. An estimate of the direction of divergence is made by analysing the SOFs estimated during the iterative process, $[SOF_{SCA}, SOF(1), \dots, SOF(u)]$. For example, in Figure 2(b) the successive estimated SOFs will increase in value. In this case, the iterative process is re-initialised by letting $\hat{SOF}(0) = SOF_{SCA} - N/4$ as shown in Figure 2(c) and then repeating the iterative process. As shown in Figure 2(d), this converges to the correct SOF in almost all cases. Obviously, the direction of divergence cannot be estimated if the iterative procedure completes with just one iteration (i.e. $u = 1$), in which case it will result in a non-convergence error being generated for ISOCA.

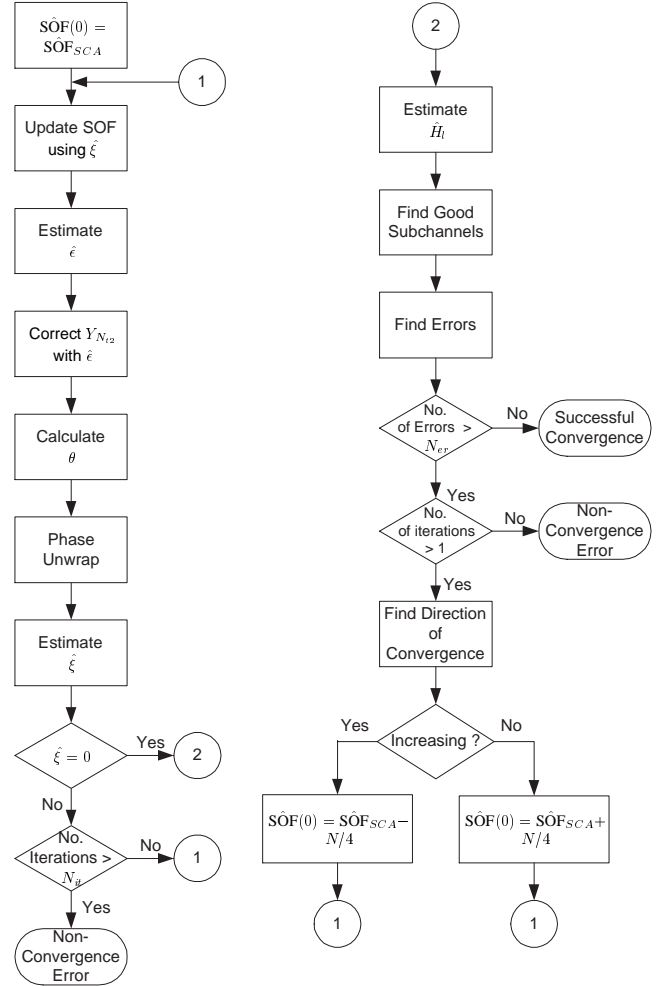


Fig. 3. ISOCA Flow Graphs: First Correction (left) Second Correction (right)

Similar scenarios apply if to begin with $\xi_{SCA} < 0$, however comments concerning $\hat{\theta}$ and $\hat{\xi}$ and the direction of adjustment is the reverse of the previous scenario. Figure 3 shows the flow graphs for the ISOCA.

V. SIMULATION PARAMETERS AND RESULTS

OFDM systems with $N = 64$ have been simulated at a sampling rate of 20 MHz with a guard interval, v equal to 20 samples and an Excess Length, $p = 10$. QPSK mapping for all subchannels has been employed and all the subchannels are used. A burst of 320000 data bits is transmitted, which takes less than 10 ms, consequently the channel is assumed constant for the duration of each burst. Each data point in the simulation results is obtained by averaging over 500 such bursts. Appropriate models for BFWA channels are in the process of being defined. The Stanford University Interim (SUI) channels comprise 6 models for 3 different terrain conditions [9]. All of them are simulated using 3-taps, each having either Rayleigh or Ricean amplitude distributions. The channel is assumed to be wide-sense stationary uncorrelated scattering (WSSUS) and each tap of the CIR is modeled as $h_i = \beta_i e^{j\phi_i}$, where the amplitude β_i and the phase ϕ_i are selected independently. We have selected the SUI-2 channel model, pertaining to terrains with low tree densities and with antennas having a directivity of 30 degrees at the SU and 120 degrees at the

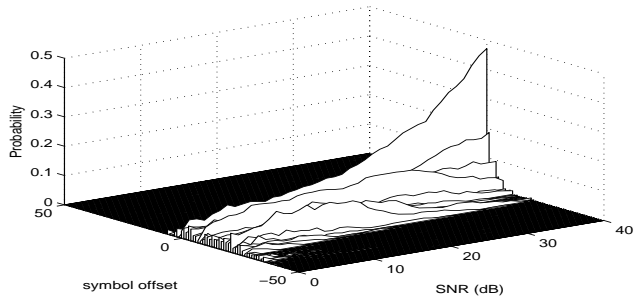


Fig. 4. Performance after SCA with AWGN and SUI-2 CIR for $N = 64$, $\epsilon = 0.5$

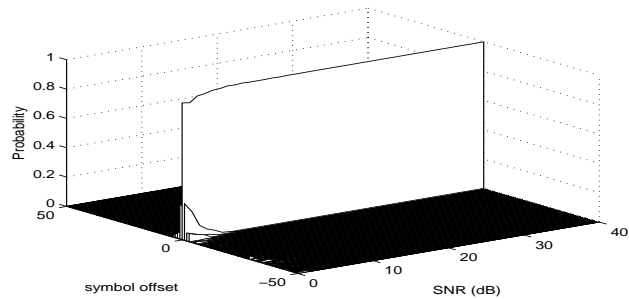


Fig. 5. Performance after 1st Correction of ISOCA with AWGN and SUI-2 CIR for $N = 64$, $\epsilon = 0.5$

BS. The channel is characterised by a RMS delay spread of 0.2 μs .

Figure 4 shows the probability of having a particular symbol offset at the end of the acquisition stage of the SCA, ξ_{SCA} for different values of SNR. It shows that in most instances ξ_{SCA} lies within an Excess Length away from SOF_{ideal} following the SCA. (i.e. the condition $-p \leq \xi_{SCA} \leq 0$ is met). The results after doing the first correction process of ISOCA are shown in Figure 5 (i.e. $\hat{\xi}(u)$ reached at the end of the first correction). This shows that the first correction is adequate for most values of SNR. However at very low SNR levels, there appears to be a low probability of $\hat{\xi}(u)$ falling beyond $N/2$ owing to the divergence of successive $\hat{\xi}$ values in the during the first part of the ISOCA, as explained in section IV. Note that after the 2nd correction of the ISOCA is applied ideal symbol synchronisation is achieved even at very low SNR values as shown in Figure 6. Figure 7 shows the comparison of the probability of failure between ISOCA and SCA. The failure rate due to non convergence of ISOCA becomes significant (i.e. defined as a probability in excess of 20%) at an SNR less than 4 dB. Note that probability of failure of SCA acquisition is not significantly better.

VI. CONCLUSION

We have presented an Iterative Symbol Offset Correction Algorithm (ISOCA), that compliments the symbol synchronisation performed by the SCA. It achieves this by iteratively tracking the phase difference between the decoded and the transmitted second training symbol of the SCA. We have shown analytically that this is possible for different ranges of the symbol offset, ξ . We have also shown through computer simulations that ISOCA performs remarkably well and achieves virtually perfect symbol synchroni-

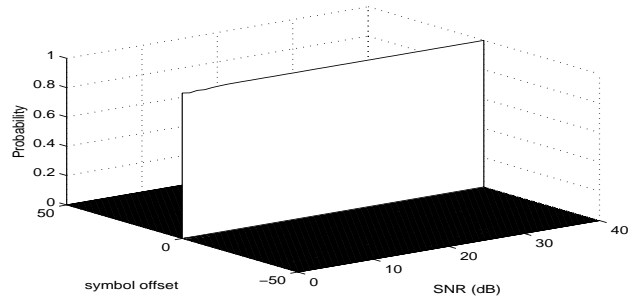


Fig. 6. Performance after 2nd Correction of ISOCA with AWGN and SUI-2 CIR for $N = 64$, $\epsilon = 0.5$

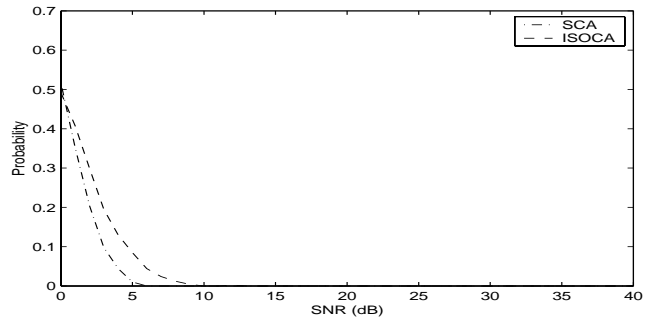


Fig. 7. Probability of no convergence with AWGN and SUI-2 CIR for $N = 64$, $\epsilon = 0.5$

ation even at very low values of SNR for OFDM systems with $N = 64$ when subjected to a SUI-2 BFWA channel model. The algorithm however has a very low but finite probability of failing to converge to the actual SOF, but this is apparent only at an SNR below 4 dB. At SNR levels that are appropriate in practical transmissions, 15-25 dB, the system works perfectly well. We hope to investigate the performance of the ISOCA with channel models other than the SUI-2 in future.

REFERENCES

- [1] T. M. Schmidl and D. Cox, "Robust frequency and timing synchronisation for OFDM," *IEEE Transactions on Communications*, vol. 45, pp. 1613–1621, December 1997.
- [2] M. Speth, F. Classen, and H. Meyr, "Frame synchronization of OFDM systems in frequency selective fading channels," in *Proceedings of the IEEE Vehicular Technology Conference*, vol. 3, pp. 1807–1811, May 1997.
- [3] J.-J. van de Beek and M. Sandell, "ML estimation of time and frequency offset in OFDM systems," *IEEE Transactions on Signal Processing*, vol. 45, pp. 1800–1805, July 1997.
- [4] T. Keller, L. Piazza, P. Mandarini, and L. Hanzo, "Orthogonal frequency division multiples synchronization techniques for frequency-selectivity fading channels," *IEEE Journal on Selected Areas in Communications*, vol. 19, pp. 999–1007, June 2001.
- [5] M. Speth, S. Fechtel, G. Fock, and H. Meyr, "Optimum receiver design for wireless broad-band systems using OFDM - part I," *IEEE Transactions on Communications*, vol. 47, pp. 1668–1677, November 1999.
- [6] V. S. Abhayawardhana and I. J. Wassell, "Residual frequency offset correction for coherently modulated OFDM systems in wireless communications," in *Proceedings of the IEEE Vehicular Technology Conference*, 2002. to be presented.
- [7] H. Minn, M. Zeng, and V. K. Bhargava, "On timing offset estimation for OFDM systems," *IEEE Communications Letters*, 2000.
- [8] H. Meyr, M. Moeneclaey, and S. Fechtel, *Digital Communication Receivers; Synchronization Channel Estimation and Signal Processing*. John Wiley & Sons Inc., 1998.
- [9] V. Erceg, K. Hari, *et al.*, "Channel models for fixed wireless applications," tech. rep., IEEE 802.16 Broadband Wireless Access Working Group, January 2001.